Science Translational Medicine
AAAS

www.sciencetranslationalmedicine.org/cgi/content/full/10/432/eaag0945/DC1

Supplementary Materials for

Obesity promotes resistance to anti-VEGF therapy in breast cancer by up-regulating IL-6 and potentially FGF-2

Joao Incio, Jennifer A. Ligibel, Daniel T. McManus, Priya Suboj, Keehoon Jung, Kosuke Kawaguchi, Matthias Pinter, Suboj Babykutty, Shan M. Chin, Trupti D. Vardam, Yuhui Huang, Nuh N. Rahbari, Sylvie Roberge, Dannie Wang, Igor L. Gomes-Santos, Stefan B. Puchner, Christopher L. Schlett, Udo Hoffmman, Marek Ancukiewicz, Sara M. Tolaney, Ian E. Krop, Dan G. Duda, Yves Boucher, Dai Fukumura,* Rakesh K. Jain*

*Corresponding author. Email: jain@steele.mgh.harvard.edu (R.K.J.); dai@steele.mgh.harvard.edu (D.F.)

Published 14 March 2018, *Sci. Transl. Med.* **10**, eaag0945 (2018)
DOI: 10.1126/scitranslmed.aag0945

This PDF file includes:

Materials and Methods

Patient data

For this study, we used data and samples from a clinical trial of bevacizumab treatment in the neoadjuvant setting in BC patients performed at Dana-Farber Cancer Institute and Massachusetts General Hospital [NCT00546156 (*24*)]. The primary study cohort was comprised of 99 patients (efficacy population). Enrollment required a pathological diagnosis of adenocarcinoma of the breast. Two cohorts of patients were eligible: patients with hormone-receptor (HR)+ tumors [virtually all HR+ tumors were estrogen receptor (ER)+] and patients with triple-negative (TN) tumors. Patients with HR+ tumors were eligible if they had high-risk disease, defined as having clinically positive axillary lymph nodes by pathological analysis, with a primary tumor ≥1.5 cm, or no evidence of axillary lymph node involvement with a high-grade tumor ≥1.5 cm, or a low/intermediate grade tumor with a primary tumor ≥2.5 cm. Patients could not have evidence of metastatic disease. Patients with bilateral cancers were eligible if at least one cancer met the eligibility requirements. Patients with TN breast cancer were required to have a tumor ≥1.5 cm. Patients with a clinically negative axilla were required to have a sentinel lymph node biopsy performed either before starting preoperative therapy or at the time of definitive surgery. For patients with a clinically positive axilla, a needle aspiration or core biopsy was required before initiation of therapy. Patients with a positive sentinel node or needle biopsy at baseline were required to undergo a level I and II axillary lymph node dissection at the time of definitive surgery. Patients received anti-VEGF as monotherapy for 14 days before initiating neo-adjuvant chemotherapy in addition to anti-VEGF. Tumor biopsies were collected at day 0 and day 14 (2 weeks of bevacizumab monotherapy), and the tumor was surgically removed at the end of the protocol. Immunohistochemistry for vessel count (CD31) and hypoxia (CA-IX) was performed on tumor samples collected on day 0 and day 14. In addition, plasma was collected at several time points (day 0, day 14, day 70, and pre-surgery around day 135), and measurements for plasma proteins were performed. The patient population was

retrospectively stratified using multiple parameters of obesity, such as BMI and amount of VAT and SAT. VAT and SAT were quantified based on CT exams of the abdomen, which were acquired as part of the clinical work-up. Using a dedicated workstation (Syngo Volume Wizard; Siemens Medical Solutions), VAT was measured in a single CT slice at the level of the umbilicus (*84, 85*). The abdominal wall muscle separating VAT from SAT was manually traced. Within the region of interest, any pixel with a CT number between -195 and -45 Hounsfield Units was defined as adipose tissue, and VAT and SAT were calculated in cm^2 (*84, 86*). Using Spearman correlation tests, we evaluated the correlation of BMI with VAT / SAT, and of obesity parameters with tumor vessels (CD31+ vessels), hypoxia (CA-IX fraction) staining, and the circulating markers IL-6 and FGF-2. Please see original clinical study (*24*) for further experimental details.

Obese mouse models

All experimental use of animals abided by the Public Health Service Policy on Humane Care of Laboratory Animals and was approved by the institutional animal care and use committee at Massachusetts General Hospital. All mice were bred and maintained in the Edwin L. Steele Laboratory gnotobiotic animal facility. C3H and C57BL/6 mice were fed either high-fat diet (HFD, composed of 60% fat, 20% protein, 20% carbohydrates based on caloric content; Research Diets D12492, irradiated) or low-fat diet (LFD, composed of 10% fat, 20% protein, 70% carbohydrates based on caloric content; Research Diets D12450J, irradiated) from 6 weeks of age until the end of the experiment, as previously described (*87, 88*). Body weight was continuously monitored. Diet-induced obese and lean states were fully established in both C57BL/6 and C3Hf/Sed mice after 8-10 weeks, at which time tumor experiments were initiated.

Tumor models

E0771 cells were originally established by Dr. F. M. Sirotnak (Memorial Sloan Kettering Cancer Center, N.Y.) and were provided by Dr. E. Mihich (Roswell Park Cancer Institute, Buffalo, NY). These cells were originally derived from a spontaneously occurring breast adenocarcinoma in C57BL/6 mice and were used to model aggressive human breast cancer cells that proliferate rapidly and metastasize to the regional lymph nodes and lungs by 4 weeks (*89*). E0771 cells were maintained in RPMI 1640 supplemented with 10% (vol/vol) fetal bovine serum (FBS, Atlanta Biologics), before being processed for protein extraction for assessment of IL-6Rα and GP130 expression. E0771 cells were authenticated in 2013 by IDEXX laboratories: "E0771: IDEXX RADIL Case # 14116-2013. The sample was confirmed to be of mouse origin and no mammalian interspecies contamination was detected. The genetic profile for this cell line contains extra alleles at 12 markers and different allele sizes at 5 markers. In addition, there are more than 2 alleles at 3 markers. The genetic profile for this cell line is not consistent with that of the C57BL/6 inbred mouse strain and is instead more consistent with having been derived from a mouse with a mixed/stock genetic background. Re-testing of this cell line after another 5-10 passages (IDEXX RADIL Case # 15518-2013) clarified that the genetic profile is intrinsic to this cell line but not likely cross-contaminated with another mouse cell line." MCaIV tumors were originally derived from a mammary adenocarcinoma that spontaneously arose in a C3H female mouse in Dr. Herman D. Suit's Laboratory at Massachusetts General Hospital (*90*). Frozen slurries of MCaIV were implanted in C3H female mice and allowed to grow until formation of tumors. Tumors were then excised and minced to generate small tumor fragments of about 1-2 mm^2 each that were subsequently used in the animal experiments in this study.

In vivo tumor experiments

After 8-10 weeks of HFD/LFD, E0771 ($1x10^6$ cells) and fragments of MCaIV were implanted orthotopically in the mammary fat pad of syngeneic immunocompetent mice (C57BL/6 and C3H mice,

respectively). For tumor implantation and collection, mice were anesthetized for 30 minutes using intramuscular injections of ketamine/xylazine (90 mg/9 mg per kg body weight). After surgery, buprenorphine 0.1 mg/kg was administered every 12 hours for 72 hours. When median tumor volume reached ~125 mm^3 (ranging from ~75 to 150 mm^3 depending on tumor model and experiment), unless otherwise noted, mice were divided into appropriate size-matched groups (equally distributing tumor size) and treated at 3-day intervals by intraperitoneal (i.p.) injection of either control rat IgG [5 mg/kg body weight (BW), Jackson ImmunoResearch Laboratories, Inc.] or the anti-VEGF antibody B20-4.1.1 (Roche/Genentech, 5 mg/kg BW). In addition, in the E0771 model, an anti-IL-6 antibody (anti-IL6*,* BioXCell, 8 mg/kg BW, i.p., doses administered at 2-day intervals) and / or the chemotherapeutic agent doxorubicin (Pfizer, 2 mg/kg BW, i.p., doses administered at 3-day intervals) were administered alone or in combination with B20-4.1.1. In the MCaIV model, the FGFR inhibitor (AZD4547, Selleckchem, 12.5 mg/kg BW per os, once daily) or metformin (Sigma, 300 mg/kg in drinking water) were administered alone or in combination with B20-4.1.1. For tumor-bearing animals, body weight was monitored at least twice per week to ensure that the mice did not experience greater than 15% decrease in body weight, at which point the animal was sacrificed. Tumor dimensions were measured by caliper every three days, and tumor volume (mm^3) was estimated using the formula: tumor volume = (long axis) $\times$ (short axis)^2 $\times$ $\pi/6$. Metastatic burden was assessed by counting lung metastases in the E0771 breast cancer model. Lungs were placed in 4% formaldehyde for 24 hours, processed for hematoxylin staining, and lung sections were obtained for visualization and counting of metastases under a light microscope. One section per lung per mouse was used, and final count per mouse represented an average of the left and right lungs.

In some experiments, control animals were sacrificed at an earlier time point than the treated groups due to the substantial effect of treatment on tumor growth. In each experiment, tumors from treated groups were collected at the same time point (time-matched). IL-6-deficient mice (*Il6*$^{-/-}$) on a C57BL/6 background were used along with age-matched WT mice. At the completion of the study, tumor samples

were collected, weighed, and processed for further analysis.

For perfusion studies, mice were injected retroorbitally with biotinylated lectin diluted in water 5 min before sacrifice. For hypoxia studies, mice were injected i.p. with 60 mg/kg of pimonidazole hydrochloride (Hypoxyprobe; Hypoxyprobe, Inc.) 45 min before sacrifice. All animals were monitored daily by the study staff, including weekends and holidays after procedures.

Metformin treatment

Standard clinical doses of metformin for adult humans range from 1000 to 2500 mg, usually given twice daily. In the present study, metformin was administered at 300 mg/kg to mice in drinking water. Using the Reagan-Shaw conversion method (*91*), we estimated that 300 mg/kg corresponds to 1459 mg for an average sized 60 kg adult human. Therefore, the selected dose is within the safe clinical therapeutic range. The amount given in the water was calculated based on the average daily water intake for a particular cage during a period of 2 weeks before treatment, and adjusted every three days based on water consumption and body weight of the animals. Drinking water was replaced every 3 days and at that time, metformin concentration in the water was adjusted for water consumption and BW of mice.

Immunohistochemistry/immunofluorescence

For immunohistochemistry of mouse samples, primary and metastatic tumor tissues were fixed in 4% (vol/vol) paraformaldehyde overnight and embedded in paraffin. Sections were stained with H&E for visualization of metastasis, mitosis, necrosis, and adipocytes, and primary tumors were stained with the antibodies included in **table S1**.

Antibody stains were counterstained with hematoxylin. Images were taken using a brightfield microscope (Olympus BX40) attached to a camera (Canon EOS 40D digital single-lens reflex camera). To quantify necrotic tumor area, 10-μm sections were stained with H&E. Tumors were evaluated, and

areas of necrosis were identified. A custom-written MATLAB (MathWorks) program was used to determine the fraction of necrotic area in the tumor:

```
% Instructions on how to use the code

% path: path of the images
%1. Open Matlab.
%2. Open up the code (areaSelection_HE_1), and set the directory as a specific folder (this should be a folder that contains all the images).
%3. Type ?areaSelection_HE_1 (?specific pathway?)? in ?command? and press enter.
%4. Now, one of the images in that specific folder will show up on the screen.
%5. To select the whole area of tumor cell, ?Left click? on the outer boundary of the tumor cell. Matlab will notice this as ?area 1.?
%6. To confirm this area, ?Right click? once outside of the box.
%7. Next, ?Left click? on the outer boundary of the viable tumor cell. Matlab will notice this as ?area 2.?
%8. To embed the area2 in area1, ?Left click? once outside of the box, and then ?Right click? once on the outside of the box. (If you have more than one ?area2?, follow the same step 8).
%9. When you are done selecting both areas, save the image file at this point.
%10. In order to move on to the next image, ?Right click? once outside of the box and then ?Right click? once inside the box.
%11. Once you finish calculating all the images, the result will be automatically appeared on the Matlab as ?Name of image, area1, area2, percentage of chosen area fraction (area2/area1)?.



function areaSelection_HE_0(path)
if ~exist('cTable','var'),   cTable=[2.^12 2.^12 2.^12];    end
if ~exist('param','var'),   param.nothing=0;    end
if ~isfield(param,'reset'), param.reset=0;  end
if ~isfield(param,'skip'), param.skip=0; end
if ~isfield(param,'display'), param.display=1; end

files=dirTiff(path);
if isempty(files)
    files=dirBMP(path);
end
if isempty(files)
    files=dirJPG(path);
end
if isempty(files)
    errordlg(sprintf('No images (JPG or Tiff or BMP) in %s',path));
```

```
    return
end

path_mat = 'mat'; path_mat=fullfile(path,path_mat);
if ~exist(path_mat,'dir'), mkdir(path_mat);   end

for f=1:numel(files)
    id = strfind(files(f).name,'.');
    ext = files(f).name(id(end):end);
    filename = strrep(files(f).name, ext, '_area.mat');
    if ( ~exist(fullfile(path_mat,filename),'file') || param.reset )
        tic;
        fn=fullfile(path,files(f).name);    visu=imread(fn);        bw=areaSelection_IHC1(visu,param);
        save(fullfile(path_mat,filename),'bw');
        t=toc;  display(sprintf('Area selection: %g/%g {%g sec}',f,numel(files),t));
    end
end

display('Filename,A1_area, A2_area, Fraction (A2/A1)');
for f=1:numel(files)
    id = strfind(files(f).name,'.');
    ext = files(f).name(id(end):end);
    filename = strrep(files(f).name, ext, '_area.mat');    load(fullfile(path_mat,filename));
    a1=bw>0;   a1_area=sum(a1(:));
    a2=bw==2;   a2_area=sum(a2(:));
    display(sprintf('%s,%g,%g,%g',files(f).name,a1_area,a2_area,a2_area/a1_area));
end

% Single Image Function
function bw=areaSelection_IHC1(visu,param)
if ~exist('param','var'),    param.skip=0;  end
if ~isfield(param,'skip'), param.skip=0; end
bw=zeros(size(visu,1),size(visu,2));

clf;
done = 0;
while (~done)
```

```
    subplot(1,2,2); imagesc(bw); axis image;    axis off;
    subplot(1,2,1); imagesc(visu); axis image;  hold on;    axis off;   title('Select Area (click outside the image to terminate selection)');
    [y x]=find(bwperim(bw)); scatter(x,y,2,[1 1 1]);
    [xi,yi,pi] = impixel;
    if isnan(pi(end))
        if ~isnan(pi(1))
            pi=pi(:,1);
            inside=find(~isnan(pi));
            class = numel(find(isnan(pi(inside(end):end))));
            roi_planebw=roipoly(size(bw,1),size(bw,2),xi(1:end-class),yi(1:end-class));
            bw(roi_planebw)=class;
        else
            if ~param.skip
                clf;
                subplot(1,2,1); imagesc(bw); axis image;
                title('ARE YOU SURE YOU ARE DONE ? (YES:CLICK INSIDE)');
                pi = impixel;
                if ~isnan(pi(1))
                    done=1;
                end
            else
                if size(pi,1)==1
                    done=1;
                end
            end
        end
    end
end



% Utility Functions
function files = dirTiff(path)
files=dir(fullfile(path,'*.TIF'));
if isempty(files),    files=dir(fullfile(path,'*.tif'));    end
if isempty(files),    files=dir(fullfile(path,'*.tiff'));   end
if isempty(files),    files=dir(fullfile(path,'*.TIFF'));   end
files=sortFilesByDate(files);
```

```
function files = dirBMP(path)
files=dir(fullfile(path,'*.BMP'));
if isempty(files),    files=dir(fullfile(path,'*.bmp'));    end
files=sortFilesByDate(files);

function files = dirJPG(path)
files=dir(fullfile(path,'*.JPG'));
if isempty(files),    files=dir(fullfile(path,'*.jpg'));    end
files=sortFilesByDate(files);

function ff = sortFilesByDate(f)
if isempty(f)
%     display('Warning: SortbyDate empty Data');
    ff=f;
    return
end
for (i=1:numel(f))
    d(i)=datenum(f(i).date);
end
[o,idx]=sort(d);
for (i=1:numel(f))
    ff(i)=f(idx(i));
end
ff=ff';
```

The majority of tumors had a viable rim; thus, the total tumor area could be determined. The area of necrosis was then quantified with respect to the full cross-sectional tumor area. To quantify adipocyte diameter, images were obtained at 4X magnification, and cross-sectional diameter was obtained using Image J software. To determine adipocyte density, sub-regions were quantitatively assessed and marked as being one of the following: adipocyte-rich – 12 adipocytes or greater per ROI; intermediate – 5 to 11; or adipocyte-poor – less than 5 adipocytes per ROI. Adipocyte density was also correlated with CD31

expression to determine the vessel density in these regions. To quantify overall CD31 expression in tumors from mouse models, slides were scanned, and analysis was performed using Aperio ImageScope. After tumors were individually manually outlined, they were analyzed using an algorithm that measures positive pixel count, as described by the manufacturer (*92*). The algorithm categorizes each pixel as being negative, weak, positive, or strong positive depending on its color and intensity. A marked up image of the annotated tumor featuring a color-coded illustration of the pixels revealed that positive and strong positive pixels corresponded to CD31 staining, whereas weak and negative pixels were representative of unstained regions. CD31 expression per tumor was calculated accordingly:

(Positive Pixels + Strong Positive Pixels)/ (Negative Pixels + Weak Positive Pixels + Positive Pixels + Strong Positive Pixels)

For human samples, bright-field images of stained slides were acquired with a Hamamatsu NanoZoomer slide scanner. Images were reviewed before analysis, and slides with clear nonspecific staining or tissue folding were excluded. CD31 quantification was performed semiautomatically using a custom software from Visiopharm, and has been described before (*24*). The software automatically detected the tissue area and areas positive for CD31 (N1596; Dako), and the automatic selection was confirmed manually by two investigators, as described below. Microvessel density was calculated for vessels that displayed at least two of the following three characteristics: positive CD31 stain, visible lumen, and elongated endothelial cell nuclei. Two entire biopsy sections, separated by 100 μm and excluding areas of adipose tissue only and nonspecific staining, were quantified and averaged for each measurement to account for spatial heterogeneity. To confirm the microvessel density results from the computer-assisted analysis, manual counting was also performed by two trained investigators and correlated with the computer analysis (Spearman's $\rho = 0.63$, $P = 0.0016$). The correlation between the two manual counts was also

tested (Spearman's $\rho = 0.74$, $P = 8.5 \times 10^{9}$). The investigators who performed the analyses were blinded to patient, treatment, and time point.

Mitotic count was performed using images obtained at 20X magnification to obtain better visualization of mitoses. Mitotic activity was assessed according to the following criteria: 1) appearance of compromised nuclear envelope indicated by discontinuous nuclear body; 2) darkened nuclear body indicating chromatin condensation; and 3) alignment of chromosomes at metaphase plate and appearance of early cytokinesis. Mitotic count was established for each ROI before calculating mean mitoses per tumor. Mean mitoses per tumor were then used to calculate mean mitoses per animal group.

For immunofluorescence, primary tumor tissues were snap frozen in liquid nitrogen, and later embedded in OCT compound. Staining was carried out on frozen sections (10 μm thick) using the antibodies described in **table S2**. Cy3-, Cy5-, FITC or streptavidin HRP conjugated secondary antibodies were used for the detection of signals by confocal microscopy. Cy5-streptavidin conjugated secondary antibody was used to detect lectin in tumor tissues. Slides were counterstained with DAPI for nuclear staining. Mosaic images of tumors were collected using an Olympus FV1000 confocal laser-scanning microscope. A 10x air objective acquired 1260-μm square tiles, and an automated stage scanned through the entire cross-section of tumor tissue. The imaged tiles were stitched into a final mosaic image using Olympus software. Antigen expression was quantified by measuring the area occupied by the stain of interest normalized to the area of DAPI-stained nuclei, and analyzed using a custom algorithm in MATLAB. Red-oil O staining was performed using a standard protocol.

Gene expression

Immediately after excision, tumor tissue was snap frozen and stored in liquid nitrogen until used. Total RNA was extracted, and relative gene expression was determined using standard RT-PCR (GLUT-1) or using RT2 Profiler PCR Arrays system (Qiagen) for PCR array on a Stratagene Mx3000P QPCR System.

The pre-made pathway-focused arrays used (mouse genes) were “Inflammatory Response and Autoimmunity” (Cat. Number: PAMM077Z), “Common Cytokines” (Cat. Number: PAMM021Z), and “Angiogenesis” (Cat. Number: PAMM024Z).

Protein expression

-Western blot analysis

Each cell or tumor sample was homogenized directly in lysis buffer for protein extraction. 20 μg of denatured protein per sample was loaded on 7%, 10%, and 12% SDS-polyacrylamide gels. Membranes were blotted with the antibodies described in **table S3**. Quantification of protein expression relative to α-tubulin, GAPDH, or ß-actin was performed using Image J software.

-ELISA/multiplex array (mouse samples)

Each tumor sample was homogenized directly in lysis buffer for protein extraction. 2 μg/μl of sample was used, and data are expressed as pg/mg of tissue protein. Plasma was obtained by centrifugation (2000 RPM for 20 minutes of peripheral blood, and data are expressed as pg/ml of plasma. A premade inflammatory multiple cytokine protein array was used for both tumor homogenates and plasma (V-PLEX Proinflammatory Panel1 mouse kit, Cat. Number K15048D). IGF-1 was measured using a mouse immunoassay (Quantikine MG-100, RD Systems). FGF-2 (basic FGF) was measured using a mouse immunoassay (Quantikine MFB00, RD Systems). VEGF-A was also measured using a mouse immunoassay (Duoset DY293B, RD Systems).

Flow cytometry analysis

Tumor-bearing mice were perfused via intracardiac injection of PBS and subsequently euthanized. Breast tumor tissues were harvested, minced, and digested at 37 °C for 1 h with Dulbecco’s modified Eagle’s Medium (DMEM) containing collagenase type 1A (1.5 mg/mL), hyaluronidase (1.5 mg/mL),

and DNase (2 mg/mL). The digestion mixtures were filtered through 70-μm cell strainers. Single-cell suspensions were incubated with rat anti-mouse CD16/CD32 mAb before being stained, washed, and resuspended in cold buffer (1% BSA, 0.1% NaN_3 in PBS). 7-amino-actinomycin D (7AAD) reagent (eBioscience) was added to the stained tubes (5 μL per tube) just before running the flow analysis. The doublet/aggregated events were gated out using forward scatter area (FSC-A) vs. forward scatter width (FSC-W) and side scatter area (SSC-A) vs. side scatter width (SSC-W). Flow cytometry data were acquired on an LSRII flow cytometer (Becton Dickinson) and analyzed using FACSDiva software. FSC-A vs. FSC-W and SSC-A vs. SSC-W were applied to discriminate the doublet/aggregated events. The appropriate fluorochrome-conjugated, isotype-matched control IgGs were used in all experiments. The monoclonal anti-mouse antibodies included in **table S4** were used in flow cytometric experiments.

Supplementary Figures

Figure S1

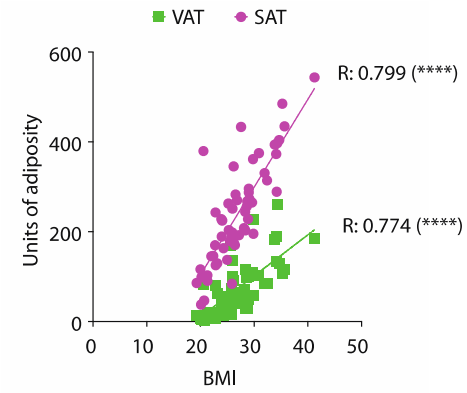

Figure S1. Correlation of VAT and SAT with BMI. Spearman's correlation coefficients between abdominal VAT / SAT (cm^2) and BMI. ****p < 0.0001. Dots correspond to individual patients. Curve represents linear regression.

Figure S2

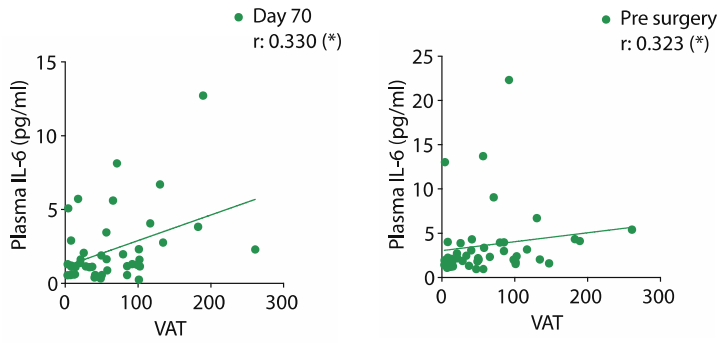

Figure S2. Correlation between plasma IL-6 and VAT at day 70 and presurgery time points. Spearman's correlation coefficients between IL-6 and VAT at day 70 (left panel) and pre-surgery (right panel). *p < 0.05. Dots correspond to individual patients. Curve represents linear regression.

Figure S3

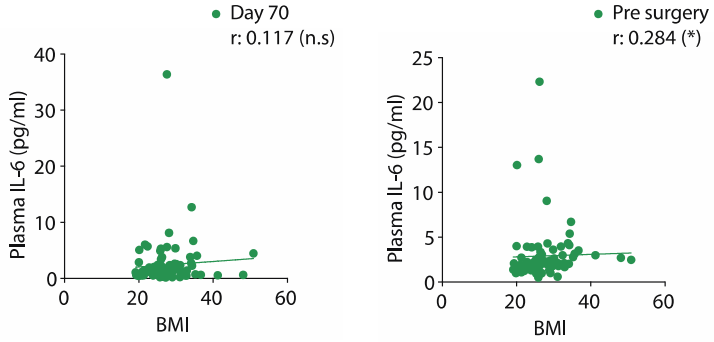

Figure S3. Correlation between plasma IL-6 and BMI at day 70 and presurgery time points. Spearman's correlation coefficients between IL-6 and BMI at day 70 (left panel) and pre-surgery (right panel). *p < 0.05. Dots correspond to individual patients. Curve represents linear regression.

Figure S4

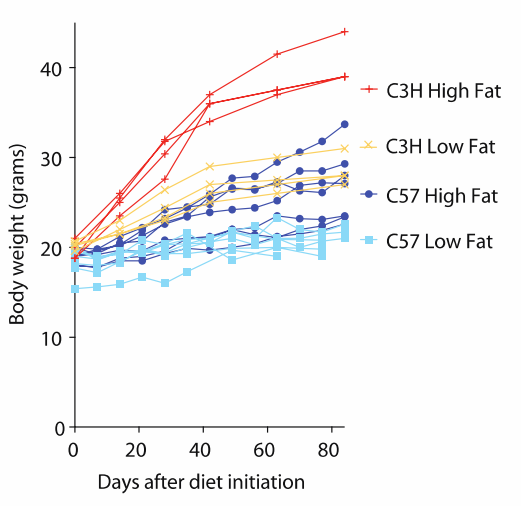

Figure S4. Individual curves of data presented in Fig. 2B. Individual body weight gain over time in C3H and C57BL/6 mice fed either a LFD or HFD.

Figure S5

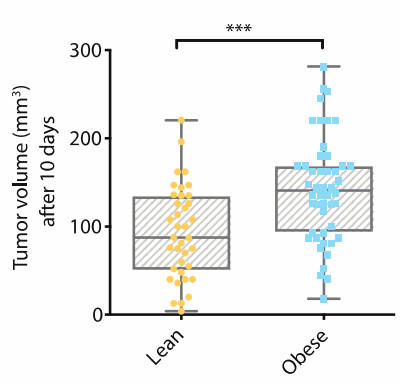

Figure S5. Correlation between obesity and tumor growth. Tumor volume data of E0771 tumors measured 10 days after implantation was aggregated from multiple cohorts of animals. Significant difference using t-test is indicated. ***p < 0.001. Data are shown as individual values plus box plots with min, max, and median values.

Figure S6

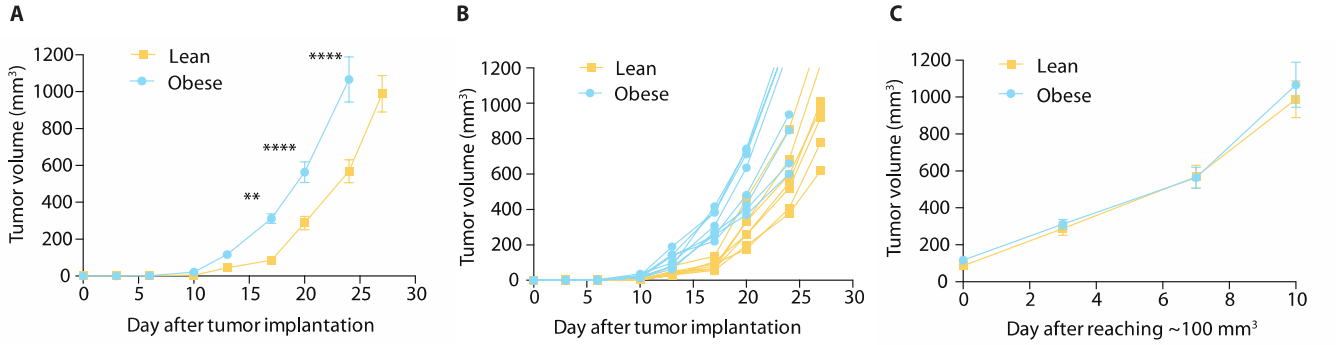

Figure S6. Early tumor progression in the setting of diet-induced obesity. (**A**) Growth curves of E0771 tumors implanted in lean and obese mice (n = 8 animals / group). (**B**) Individual growth curves of data presented in (A). **(C)** Same data as in (A), plotted by matching tumor size at ~125 mm^3 at day 0. Significant differences using two-way ANOVA with post hoc multiple comparisons test are indicated in A and C. **p < 0.01, ****p < 0.0001. Data in panels A and C are presented as mean ± SEM.

Figure S7

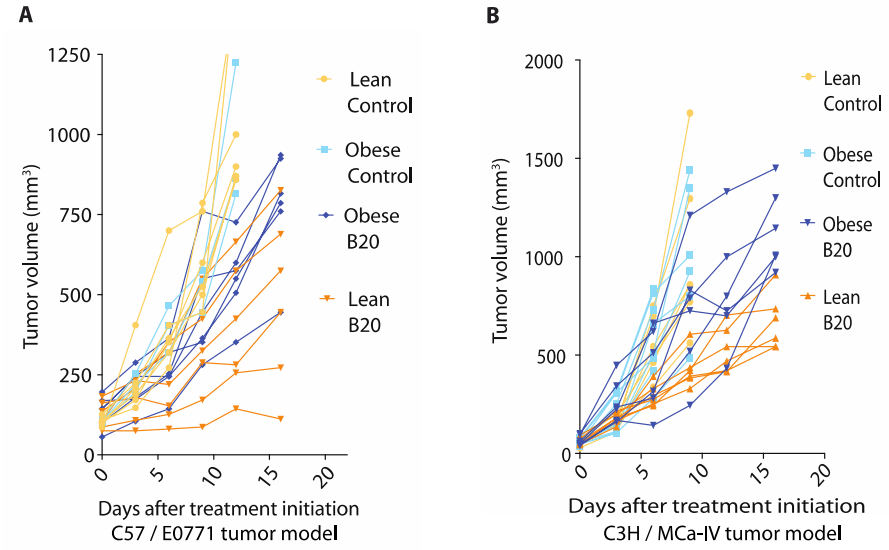

Figure S7. Individual curves of data presented in Fig. 2 (D and E). E0771 **(A)** and MCaIV **(B)** tumor growth in obese versus lean mice treated with control IgG or anti-VEGF antibody (B20).

Figure S8

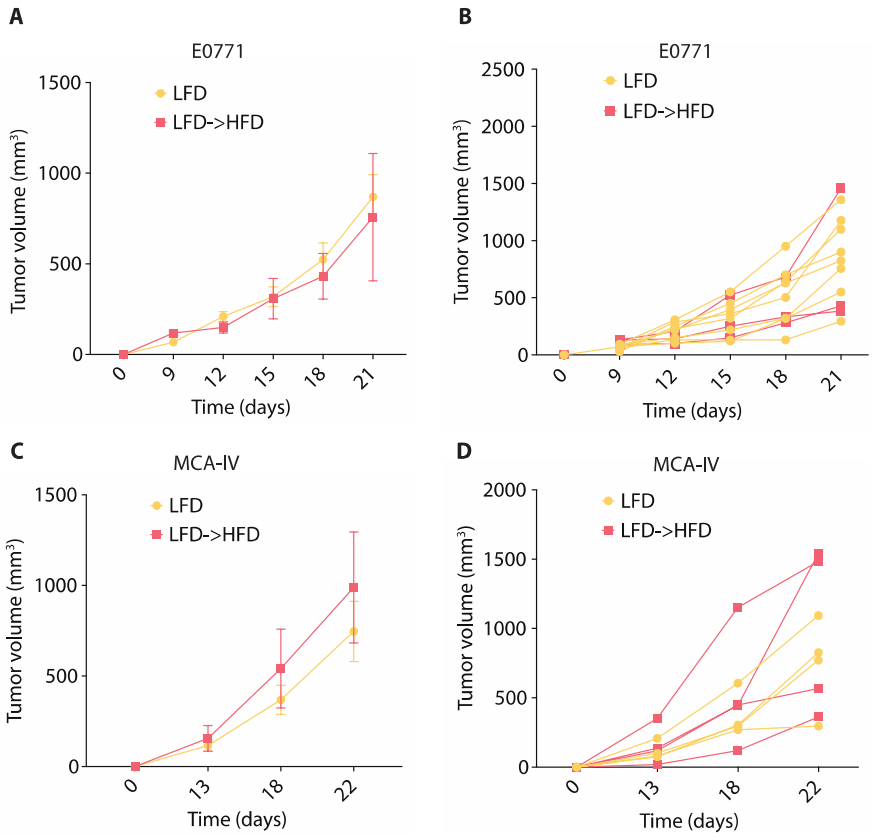

Figure S8. Tumor progression influenced by BW but not diet. (A-D) Mice were put on a low-fat diet for 10 weeks. Breast tumors were then orthotopically implanted, and some of the mice were maintained on low-fat diet while others switched to a high-fat diet (E0771: LFD, n = 7; LFD => HFD, n = 3. Two additional animals in the latter group were excluded due to failure of tumor growth. MCaIV: LFD, n = 4; LFD => HFD, n = 4). Graphs depict tumor growth curves for E0771 (A, individual curves in B) and MCaIV (C, individual curves in D) tumors.

Two-way ANOVA was used to determine significant differences. Data in panels A and C is presented as mean ± SEM.

Figure S9

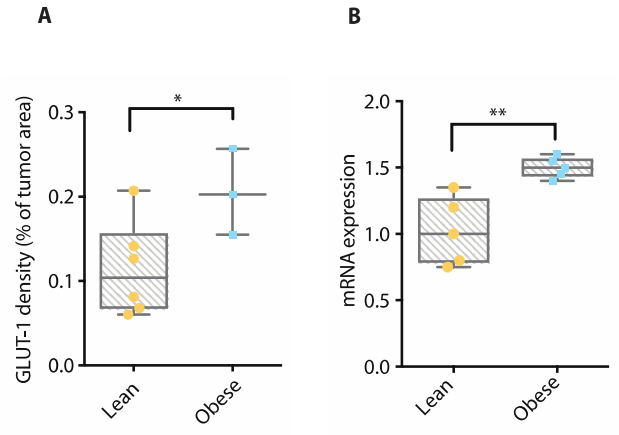

Figure S9. Association between obesity and expression of the hypoxia marker GLUT-1. (**A-B**) Quantification of GLUT-1 tissue expression (immunofluorescence in A, staining as a percentage of DAPI positive viable area) and mRNA expression (B) in E0771 tumors from lean and obese mice. Significant differences using t-test are indicated, *p < 0.05, **p < 0.01. Data are shown as individual values plus box plots with min, max, and median values.

Figure S10

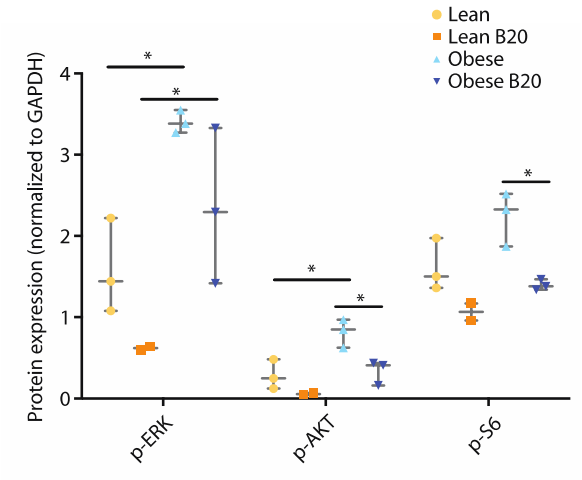

Figure S10. Quantification of Western blot data presented in Fig. 3C. Quantification of protein expression normalized to GAPDH in tumors from lean and obese animals treated with control IgG or B20. Significant differences using two-way ANOVA with post hoc test for multiple comparisons are indicated, *p < 0.05. Data are shown as individual values plus box plots with min, max, and median values.

Figure S11

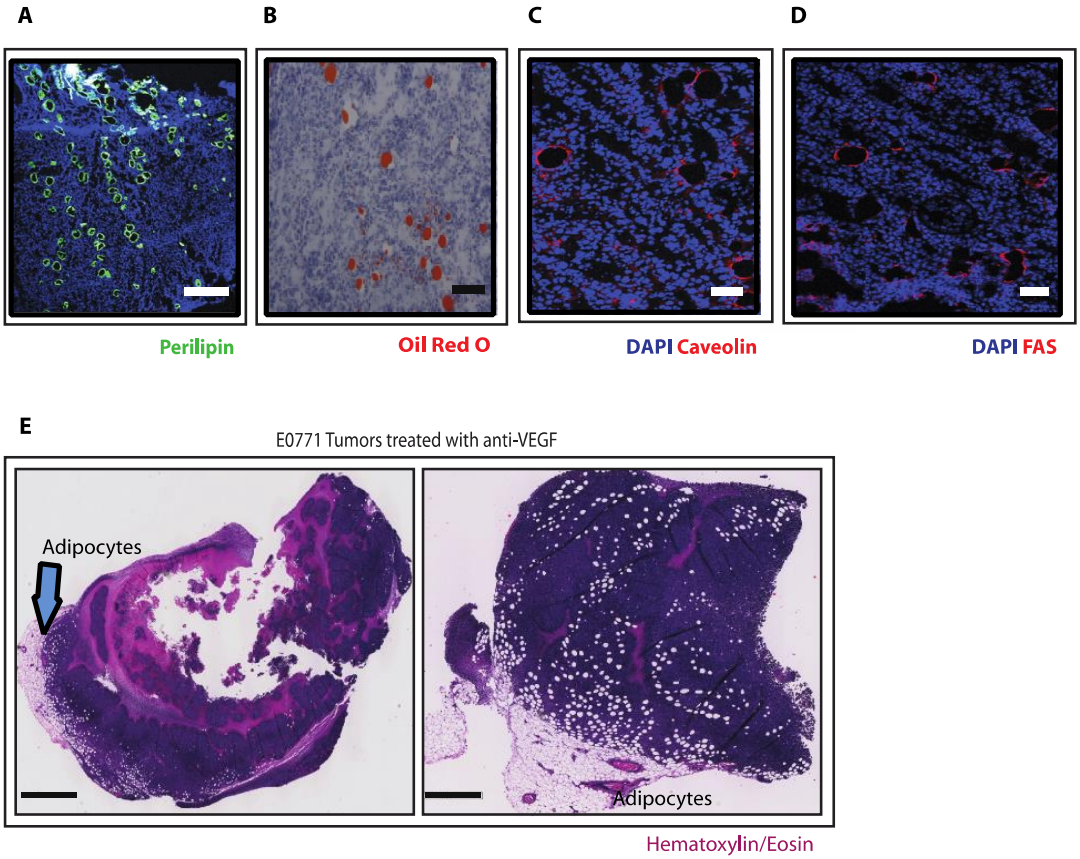

Figure S11. Detection and location of adipocytes in tumors. (A-D) Detection of adipocytes in E0771 tumor sections. Representative images of (A) perilipin, (B) Oil Red O staining, (C) caveolin, and (D) fatty acid synthase (FAS) staining in E0771 tumors. Scale bars: 300 μm (A), 200 μm (B-D). (**E**) Additional H&E stained sections of E0771 tumors from animals treated with anti-VEGF. Arrow points to adipocytes. Scale bars: 1 mm.

Figure S12

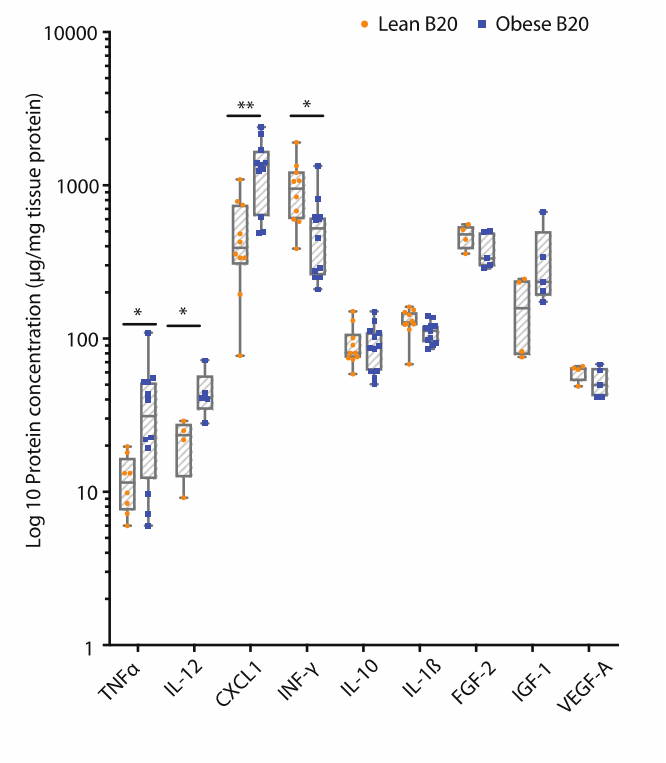

Figure S12. Expression of additional inflammatory and angiogenic markers in tumors from lean and obese mice treated with B20. Protein expression of proinflammatory cytokines and proangiogenic growth factors in E0771 tumors from lean and obese animals treated with B20. Significant differences using t-test are indicated, *p < 0.05, **p < 0.01. Data are shown as individual values plus box plots with min, max, and median values.

Figure S13

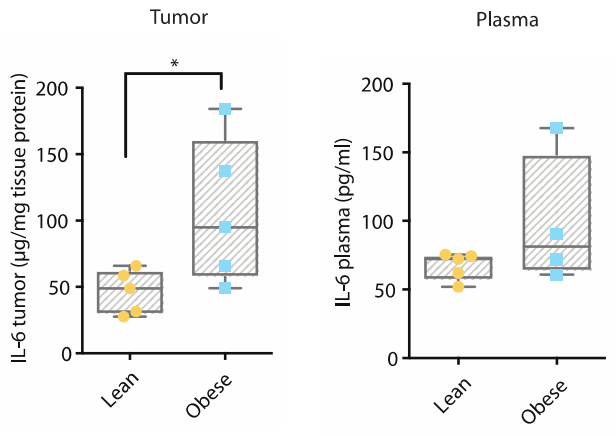

Figure. S13. Association between obesity and increased concentrations of tumor IL-6. Plasma and tumor concentration of IL-6 in E0771 tumor-bearing lean and obese mice. Tumors were orthotopically implanted in lean or obese mice, and both tumors and plasma were collected 2 weeks after. Significant differences using t-test are indicated, *p < 0.05. Data are shown as individual values plus box plots with min, max, and median values.

Figure S14

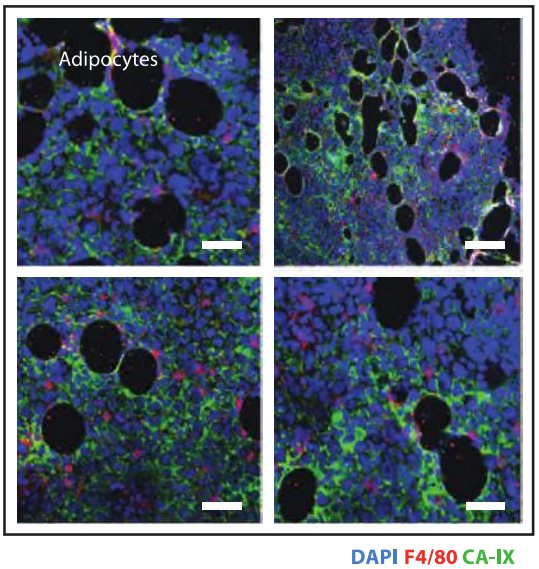

Figure S15

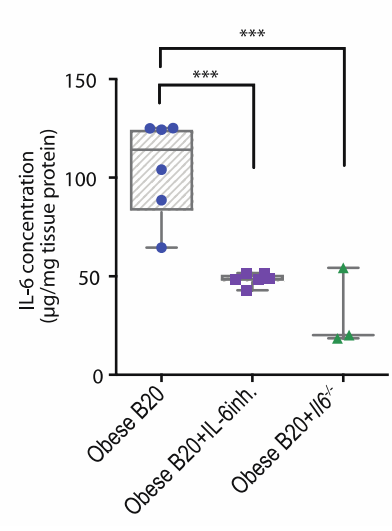

Figure S14. Additional representative immunofluorescence stains of F4/80 and CA-IX in E0771 tumors. Scale bars: 150 µm (upper left and bottom panels), 300 µm (upper right panel).

Figure S15. Decreased concentration of tumor IL-6 after pharmacological or genetic inhibition in anti-VEGF–treated mice. Concentration of IL-6 in E0771 tumors from B20-treated mice vs B20 plus IL-6 pharmacological inhibition vs. B20-treated *Il6*$^{-/-}$ mice. Mice were treated as in Fig. 6A. Significant differences using one-way ANOVA with post hoc multiple comparisons tests are indicated, ***p < 0.001. Data are shown as individual values plus box plots with min, max, and median values.

Figure S16

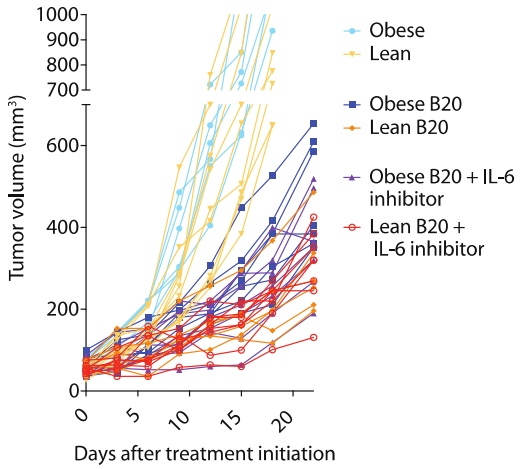

Figure S16. Individual tumor growth curves of data presented in Fig. 6A. E0771 tumor growth in obese versus lean mice treated with control IgG, anti-VEGF antibody (B20), or the combination of B20 with IL-6 inhibition.

Figure S17

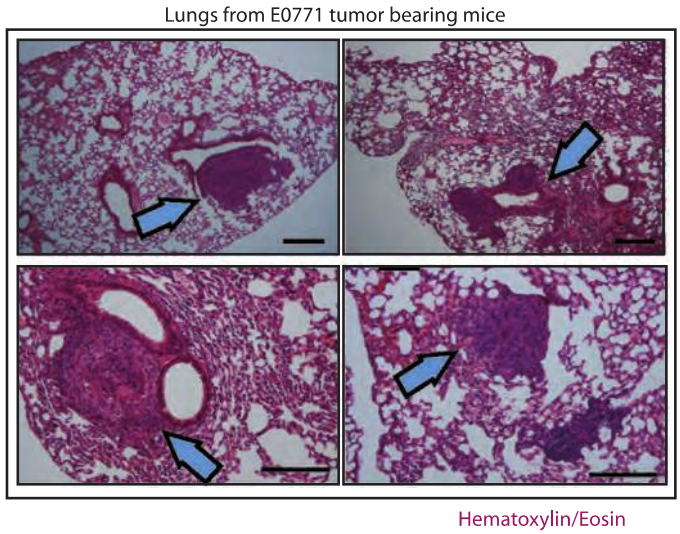

Figure S17. Additional images of lungs from mice implanted with E0771 tumors. Hematoxylin and eosin stains of lungs affected with metastasis (arrows) from E0771 tumor-bearing mice treated with B20. Scale bars: 600 µm (top); 300 µm (bottom).

Figure S18

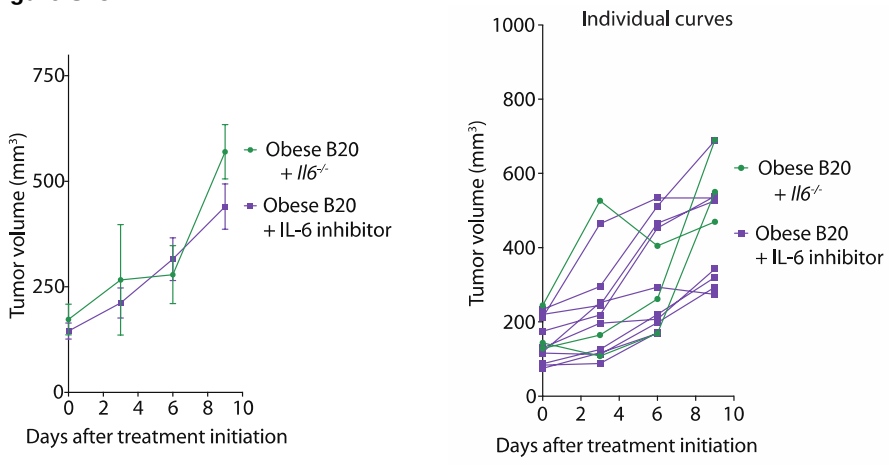

Figure S18. Similar effects of pharmacological and genetic inhibition of IL-6 on tumor growth in animals treated with anti-VEGF (B20). Two-way ANOVA was used for statistical analysis (obese B20 + IL-6 inhibitor, n = 10; obese B20 + IL-6$^{-/-}$, n = 3). Data are shown as mean ± SEM (left panel) and individual tumor growth curves (right panel).

Figure S19

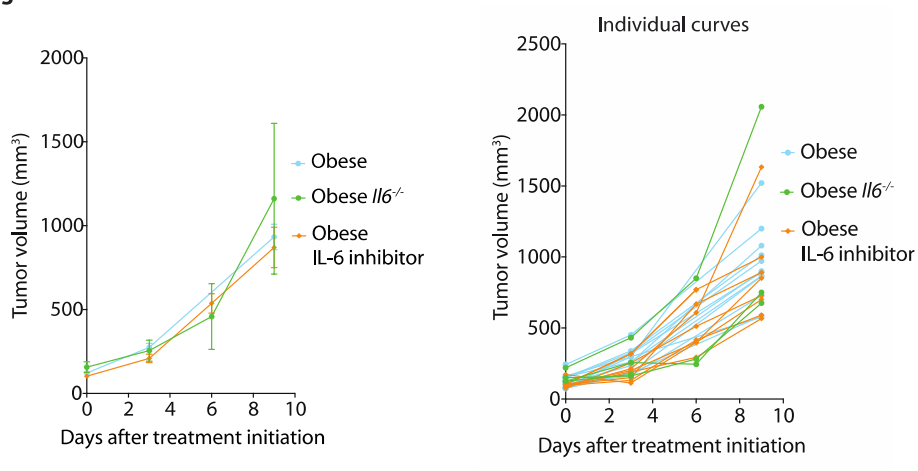

Figure S19. No effect on tumor growth after pharmacological or genetic inhibition of IL-6 alone in obese mice. Two-way ANOVA was used for statistical analysis (obese, n = 12; obese IL-6 inhibitor, n = 9, obese IL-$6^{-/-}$, n = 4. One animal in the latter group was found dead on day 6). Data are shown as mean ± SEM (left panel) and individual tumor growth curves (right panel).

Figure S20

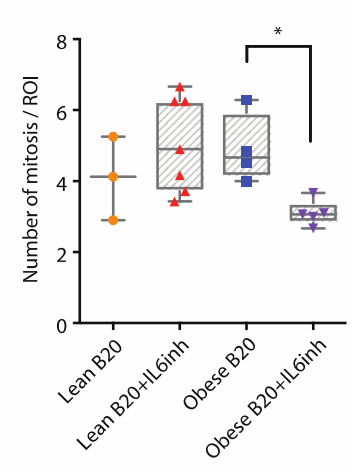

Figure S20. Reduced mitotic count with IL-6 inhibition in E0771 tumors from obese mice treated with B20. Mitotic count per region of interest in tumors from lean and obese animals treated with B20 or B20 plus IL-6 inhibition. Tumor sections were stained for hematoxylin and eosin to reveal mitotic cells. Significant differences using two-way ANOVA with post hoc multiple comparisons tests are indicated, *p < 0.05. Data are shown as individual values plus box plots with min, max, and median values.

Figure S21

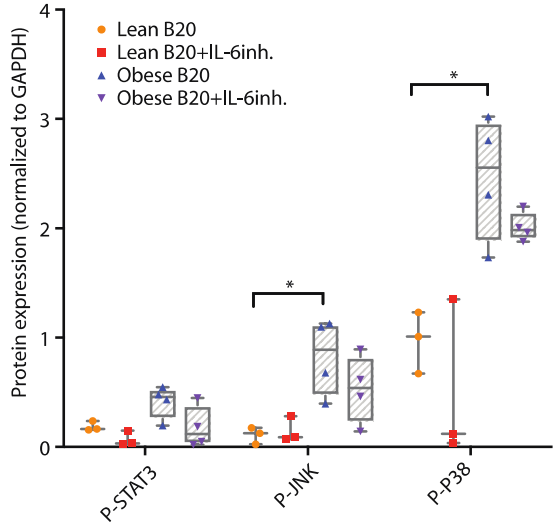

Figure S21. Quantification of Western blot data presented in Fig. 6D. Quantification of protein expression normalized to GAPDH in tumors from lean and obese animals treated with B20 or B20 plus IL-6 inhibition. Significant differences using two-way ANOVA with post hoc test for multiple comparisons are indicated, *p < 0.05. Data are shown as individual values plus box plots with min, max, and median values.

Figure S22

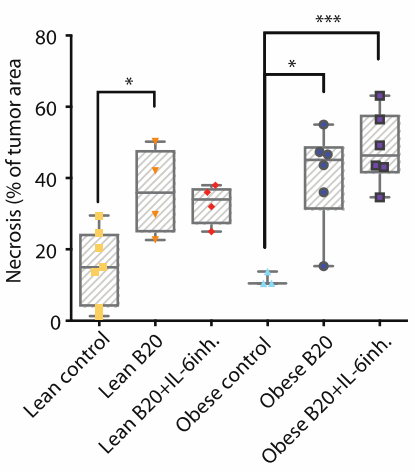

Figure S22. Tumor necrosis induced by B20. Quantification of necrosis in E0771 tumors from lean and obese animals treated with control IgG, B20, or B20 plus IL-6 inhibition. Tumor sections were stained with hematoxylin and eosin for quantification of necrotic areas. Significant differences using two-way ANOVA with post hoc multiple comparisons tests are indicated, *p < 0.05, ***p < 0.001. Data are shown as individual values plus box plots with min, max, and median values.

Figure S23

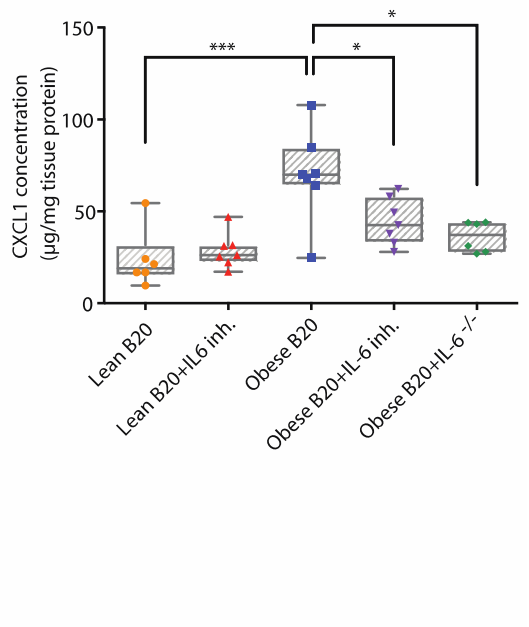

Figure S23. Reduced concentration of tumor CXCL1 in obese mice treated with B20 and IL-6 inhibition. Significant differences using one-way ANOVA with post-hoc multiple comparisons tests are indicated, *p < 0.05, ***p < 0.001. Data are shown as individual values plus box plots with min, max, and median values.

Figure S24

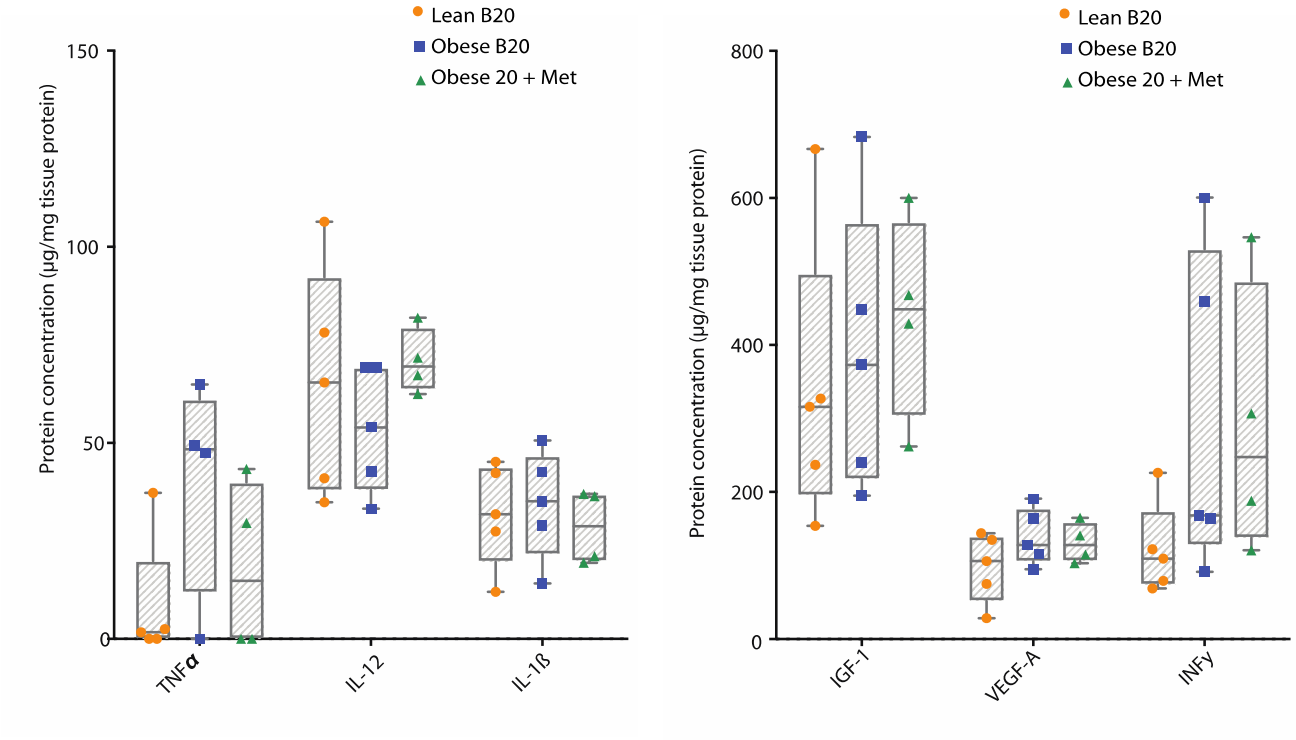

Figure S24. Expression of additional inflammatory and angiogenic markers in MCaIV tumors from lean and obese mice treated with B20 or obese mice treated with B20 plus metformin. Significant differences were assessed with one-way ANOVA. Data are shown as individual values plus box plots with min, max, and median values.

Figure S25

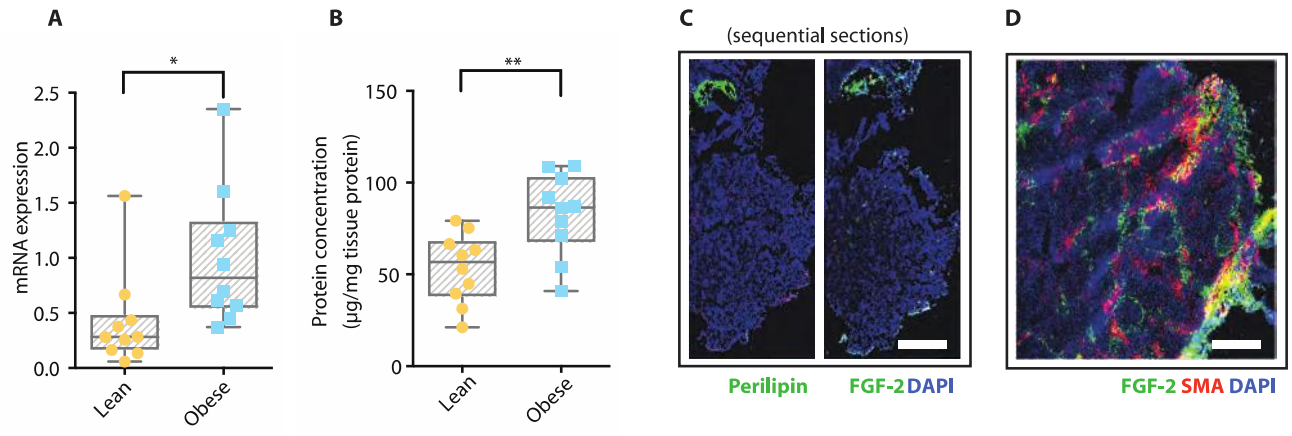

Figure S25. Association of obesity and increased FGF-2 expression in tumors, particularly around adipocytes and fibroblasts. (A) mRNA expression of *Fgf-2* in MCaIV tumors from lean and obese animals. **(B)** Protein expression of FGF-2 in MCaIV tumors from lean and obese animals. **(C)** Sequential staining for perilipin (adipocyte marker) and FGF-2 in tumor samples. **(D)** Co-staining of SMA (fibroblast marker) with FGF-2 in tumor samples. Scale bars: 600 µm. Significant differences for A-B using t-test are indicated, * $p < 0.05$, ** $p < 0.01$. Data in A-B are shown as individual values plus box plots with min, max, and median values.

Figure S26

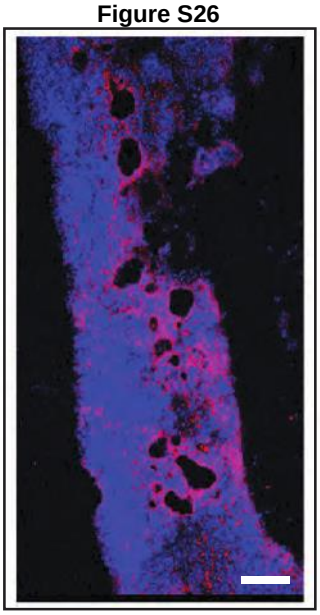

Figure S27

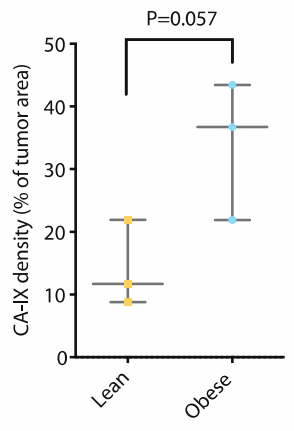

Figure S28

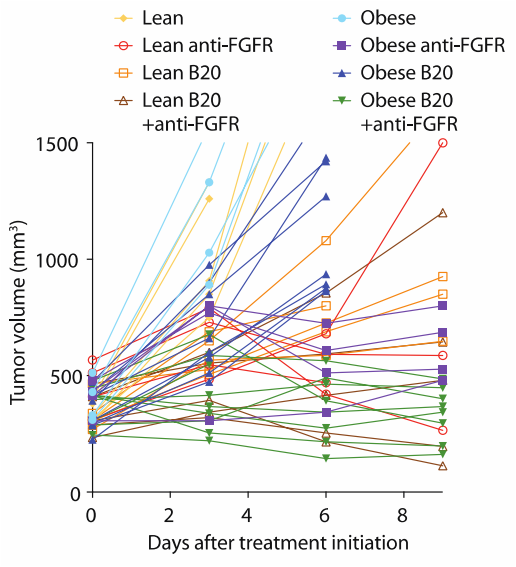

Figure S29

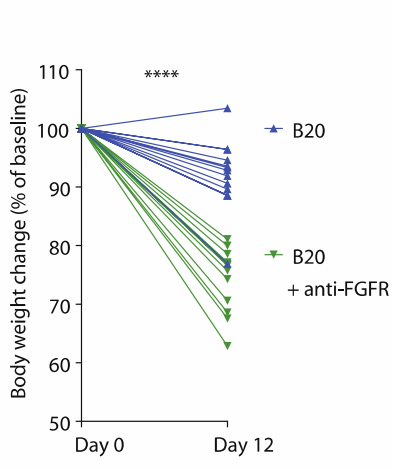

Figure S26. CA-IX expression near adipocytes in MCaIV tumors. Representative picture of CA-IX expression surrounding adipocytes. Scale bar: 300 µm.

Figure S27. Effect of obesity on CA-IX expression in MCaIV tumors. Quantification of CA-IX expression in tumors. P value using t-test is indicated. Data are shown as individual values plus box plots with min, max, and median values.

Figure S28. Individual tumor growth curves of data presented in Fig. 7E. Data correspond to MCaIV tumor growth in lean and obese mice treated with IgG, B20, anti-FGFR, or a combination of B20 with anti-FGFR.

Figure S29. Decreased BW after FGFR inhibition in tumor-bearing mice treated with B20. MCaIV tumor-bearing C3H mice were treated with B20 (n = 14 animals / group) or B20 + FGFR inhibition (n = 13 animals / group) for 12 days. Body weight was measured at baseline at day 12. Significant differences using two-way ANOVA are indicated, ****$p < 0.0001$. Data are shown as individual body weight curves.

Figure S30

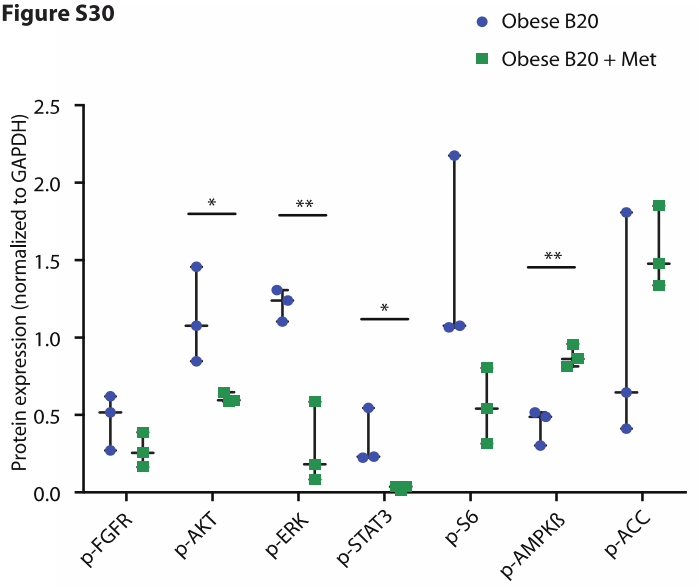

Figure S30. Quantification of Western blot data presented in Fig. 7F. Quantification of protein expression normalized to ß-actin in tumors from obese animals treated with B20 or B20 plus metformin. Significant differences using t-test are indicated, *$p < 0.05$, **$p < 0.005$. Data are shown as individual values plus box plots with min, max, and median values.

Supplementary Tables

Table S1. Antibodies used for immunohistochemistry.

Antigen	Dilution	Catalog #	Vendor
IL-6	1:200	6672	Abcam
FGF-2	1:200	(147): sc-79	Santa Cruz
CD31-biotin	1:200	DIA310	DiANOVA
CA-IX	1:200	15086	Abcam

Table S2. Antibodies used for immunofluorescence.

Antigen	Dilution	Catalog #	Vendor
Fatty Acid Synthase	1:50	3180	Cell Signaling
F4/80-biotin	1:100	MCA497A488	Serotec
Ki67	1:100	15580	Abcam
IL-6	1:200	ab6672	Abcam
GLUT-1	1:200	652	Abcam
CA-IX	1:200	15086	Abcam
CD11b-biotin	1:200	553309	BD Pharmingen
Perilipin	1:200	9349	Cell Signaling
p-STAT3^{Tyr705}	1:200	9145	Cell Signaling
FGF-2	1:200	(147): sc-79	Santa Cruz
CD31	1:200	MAB1398Z	Millipore
Caveolin	1:400	3238	Cell Signaling
αSMA-Cy3	1:500	C6198	Sigma

Table S3. Antibodies used for Western blotting.

Antigen	Dilution	Catalog #	Vendor
p-AKT^{Ser473}	1:1000	4060	Cell Signaling
p -p38MAPK$^{T180/Y182}$	1:1000	4511	Cell Signaling
p-pS6$^{Ser235/236}$	1:1000	4857	Cell Signaling
p-STAT3^{Tyr705}	1:1000	9145	Cell Signaling
p-ERK(p44/42MAPK)$^{T202/Y204}$	1:1000	4370	Cell Signaling
p-JNK(SAPK/JNK)$^{Thr183/Tyr185}$	1:500	4668	Cell Signaling
p-FGFR^{Tyr463}	1:1000	bs-5326R	Bioss
p-ACC^{Ser79}	1:1000	3661	Cell Signaling
p-AMPK β ^{Ser108}	1:1000	4181	Cell Signaling
IL-6Rα	1:100	AF1830	R&D
GP130	1:100	BAM4681	R&D
ERα	1:1000	75635	Abcam
ERβ	1:1000	5513	Cell Signaling
HER2/ERBB2	1:1000	2242	Cell Signaling
α -tubulin	1:2000	T5168	Sigma
β-actin	1:5000	4970	Cell Signaling
GAPDH	1:2000	2118	Cell Signaling

Table S4. Antibodies used for flow cytometry.

Antigen	Conjugate	Catalog_#	Vendor
CD4	FITC	553047	BD
	PECy7	100528	Biolegend
CD45	PE	103106	Biolegend
	PECy7	552848	BD
CD25	APCCY7	102026	Biolegend